Global Journal of Pure and Applied Mathematics.
ISSN 0973-1768 Volume 18, Number 1 (2022), pp. 583-612

http://www.ripublication.com/gjpam.htm

Hydromagnetic Surface Driven Flow Between Two Parallel Vertical Plates in the Presence of Chemical Reaction and Induced Magnetic Field

Jumanne Mng'ang'a
Pan African University Institute for Basic Sciences, Technology and Innovation, Kenya
Mathew Kinyanjui
Jomo Kenyatta University of Agriculture and Technology, Kenya
Edward Richard Onyango
Jomo Kenyatta University of Agriculture and Technology, Kenya

Abstract

This paper examines an unsteady hydromagnetic surface driven flow between two parallel vertical plates in presence of chemical reaction and induced magnetic field is studied. The governing equations are continuity equation, equation of momentum, energy equation, concentration equation and magnetic induction equation. The model used for the surface driven/Couette flow incorporates the effects of Soret and Dufour. The system of nonlinear partial differential equations governing the flow are solved numerically by applying numerical approximation finite difference method and implemented in MATLAB. The numerical solutions are displayed graphically and discussed, while numerical values of variations in Skin-friction, Nusselt number and Sherwood number at the plate are computed using MAPLE program and represented in tabular form. The findings of this study are important due to its application in developing a variety of chemical technologies, including polymer manufacturing, chemical catalytic reactors and food processing. The findings are found to be in an excellent agreement.

keywords Couette flow ; MHD ; Chemical reaction ; Variable magnetic field ; FDM

1 Introduction

Couette flow can be defined as the laminar flow of a viscous fluid between two parallel surfaces, one of which moves tangentially relative to the other due to drag force acting on the fluid, which can be motivated by a pressure gradient provided in the flow direction. The Couette flow is important in lubrication, polymer production and food processing

was analyzed by Demirel [1]. Hydromagnetic Couette flow is an intriguing topic that has gotten a lot of attention due to its applications in engineering and science. For example in MHD power generators (the use of potassium-seeded coal combustion gas in MHD power generation showed potential for increased energy conversion efficiency), Astrophysics (the MHD is applicable in astrophysics, including stars, the interplanetary medium , and possibly the interstellar medium , as well as jets) and Geophysical fluid dynamics (geophysical fluid dynamics is used to study large-scale flows in the earth's atmosphere, oceans, and other ecosystems).

The study on hydromagnetic surface driven or couette flow between two parallel vertical plates has been carried out by various researchers. Couette flow have been published such as Soundalgekar [2] studied transverse magnetic field with steady MHD Couette . It was concluded that velocity gradient, skin-friction and velocity profiles at the upper wall are affected by the rarefaction of the gaseous medium. Soundalgekar [3] discussed conducting walls in slip-flow regime with Heat transfer in MHD couette flow. Soundalgekar et al. [4] described the influence of hall and ion-slip with heat transfer. They are observed that when the Hartmann number is small and the Hail and Ion Slip parameters are large, or when the Hartmann number is large, the flow may become unstable. Mandal and K. Mandal [5] studied conducting plate in a rotating system with the effect of hall current. Soundalgekar and Uplekar [6] described hall effects in MHD Couette flow with heat transfer. They concluded that axial magnetic field decreases with increasing hall current and the symmetry of the transverse induced magnetic field is disturbed due to an increase in hall current. Bodosa and Borkakati [7] analyzed uniform transverse magnetic field with heat transfer for two horizontal plates . They are observed that near the plates, the velocity distribution increases, then slowly decreases between the two plates. Alabraba et al. [8] presented variable wall temperature for two-component plasma. They concluded that When both walls are conducting or not conducting, the Nusselt number increases slowly with the Hartmann number at the walls, but when one wall is conducting and the other is not conducting, the Nusselt number increases abruptly at the non conducting walls and steadily at the other wall.

Seth et al. [9] analyzed an inclined magnetic field in a rotating system. Umavathi et al. [10] analyze the inclined channel for Poiseuille-Couette flow with heat transfer. They concluded that increases in the angle of inclination, Grashof number and height ratio increase velocity, while increases in the viscosity, Hartmann number and conductivity ratios suppress velocity. The relevant parameters have an inverse effect on the lower plate Nusselt number Attia [11] investigated viscoelastic fluid with heat transfer.

Jha and Apere [12] investigated flows in an annuli with unsteady MHD couette by using Riemann-sum approximation . Bég et al. [13] analyzed oblique magnetic field in a rotating highly permeable medium. They indicated that the primary and secondary flows are both accelerated by raising the magnetic field inclination. Increasing the Darcy number also speeds up both the main and secondary flows. In the transitory instance, raising the inverse Ekman number is connected with increased primary flow reversal up to a threshold amount, beyond which it is reduced. However, when the Ekman number climbs, the secondary flow accelerates and flow reversal never occurs. Attia and Sayed-Ahmed [14] analyzed couette flow of a casson fluid with heat transfer. It was concluded that in the x-direction, the Hall term impacts the main velocity component u, and in the

z-direction, it causes another velocity component w.

Attia et al. [15] analyzed the dusty fluid with exponential decrease in the pressure gradient. The velocity distributions for both the fluid and dust particles are obtained by solving the equations of motion analytically. They found that the magnetic field's effect on the temperatures of the fluid and particles varies over time. Also, the suction velocity has a stronger effect on velocity and temperature than the magnetic field. Guo and Leong [16] analyzed perfectly conducting walls and cylindrical porous annulus . They concluded that when the external magnetic field strength is increased, the flow becomes more uniform; when the permeability of the porous medium decreases, the magnetic fluid slows. Barikbin et al. [17] analyzed non-Newtonian fluid for MHD Couette flow using the Ritz-Galerkin method .They concluded that the Ritz Galerkin approach in Bernstein polynomial and the Collocation method are both effective in solving nonlinear problems in non-Newtonian fluid mechanics. Non-linearity is not a major issue for Ritz Galerkin method in Bernstein polynomial method when compared to other numerical techniques such as finite differences.

Sreekala and Reddy [18] studied the effect of inclined magnetic field with steady MHD couette flow. The velocity and the temperature are evaluated by using perturbation technique. They concluded that the rate of surface Heat transfer (Nusselt number) improves with Reynolds number, suction parameter, Darcy parameter, Prandtl number, and Eckert number while decreasing with increasing magnetic parameter. Joseph et al. [19] investigated heat transfer in inclined magnetic field with unsteady MHD Couette flow between two infinitely parallel porous plates. They are observed that the velocity as well as the skin friction reduces as the Hartmann number rises. When the magnetic field is strong, the energy loss through the plates is reduced. Larger Nusselt numbers, on the other hand, indicate more vigorous convection. Furthermore, when the Prandlt number rises, the temperature distribution falls.

The temperature-dependent transient MHD couette flow and heat transfer of dusty fluid was studied by Mosayebidorcheh et al. [20] Jha et al. [21] investigated thermal radiation with unsteady MHD free convective Couette flow. The magnetic fields lines to the moving upper plate was investigated by Onyango et al. [22] Vyas and Srivastava [23] investigated symmetric convective cooling inside a composite duct with an entropy. They concluded that with an increase in Biot number , thermal conductivity ratio, Brinkman number, porous layer thickness, and Hartmann number , the temperature in the channel rises.The temperature, on the other hand, drops as the Biot number rises.

Ali et al. [24] discussed nano fluids in a rotating system under the influence of hall current. They concluded that the flow system is significantly influenced by hall current.Also they found that increasing the hall current parameter has a negative effect on the primary induced magnetic field, but it has a positive effect on the secondary induced magnetic field. Kiema et al. [25] investigated uniform transverse magnetic field with steady MHD couette flow. They indicated that when the magnetic inclination and Hartmann number increase, the velocity profile will decrease. Ngiangia and Okechukwu [26] discussed the impact of radiation and variable electroconductivity. They indicated that increases in electroconductivity ,Prandtl number, Reynolds number, and Grashof number result in an increase in velocity distribution, while increases in magnetic field result in a drop in velocity. Raju et al. [27] discussed natural convection Couette flow under the influence of

diffusion thermo and thermal diffusion using finite element method. Ali et al. [28] investigated convective cooling of the nanofluids in a rotating system. They concluded that with an applied magnetic field, the primary velocity increases near the stationary plate and decreases near the moving plate, whereas the secondary velocity decreases as the magnetic field increases. Job and Gunakala [29] studied the thermal radiation for vertical permeable plates using Galerkin's finite element method. They concluded that increases in the radiation parameter resulted in a drop in velocity profiles over short periods of time, but an increase over longer periods of time. As the Prandtl number, Eckert number, and Reynolds number increased, so did the temperature and velocity profiles.

Also Ali et al. [30] analyzed Couette flow of a maxwell fluid for three dimensional with periodic injection/suction. They concluded that the Hartmann number is a control mechanism for skin friction along the primary flow direction. Kamran and Siddique [31] analyzed the third grade fluid for MHD couette and poiseuille flow Kimathi et al. [32] discussed influence of the direction of a transverse magnetic field , suction and injection. Hussain et al. [33] analyzed instability of MHD couette flow of an electrically conducting fluid. They concluded that the magnetic field's effect on the shape of the undisturbed velocity profile, which is solely dependent on the Hartmann number, is the determining factor. To discover the eigenvalue problem, the stability equations were solved with the QZ-algorithm. The numerical results reveal that a magnetic field of a certain magnitude destabilizes Couette flow, but a magnetic field of a different magnitude stabilizes it. The two-step exothermic chemical reaction with thermal criticality and entropy generation of generalized Couette hydromagnetic flow was presented by Kareem and Gbadeyan [34]. Anyanwu et al. [35] discussed the influence of radioactive and a constant pressure gradient on unsteady MHD Couette flow. It has been discovered that when the pressure gradient increases, the primary velocity increases, while the radiation parameter increases, the thermal profile of the flow decreases. Numerically, thermal radiation effects on MHD Couette flow of a fuzzy nanofluid was investigated by Siddique et al. [36]. They concluded that the use of solid particle frictions improves heat transfer, while a large estimate of a magnetic parameter reduces the velocity component.

Akgül and Siddique [37] described analysis of MHD Couette flow by fractal-fractional differential operators. Sharma et al. [38] analyzed the production of entropy in a heat source-influenced thermal radiative oscillatory MHD couette flow. They concluded that entropy generation may be controlled or reduced by changing the heat radiation and applied magnetic field. Owuor [39] investigated two vertical semi-infinite permeable plates with hydromagnetic Couette flow. They concluded that increased Reynolds number causes the primary and secondary flow velocity to increase, while increased suction and injection parameters cause the primary flow to decrease.

The dusty fluid with transient generalized Taylor-Couette flow using semi analytical approach was discussed by Jha and Danjuma [40]. Numerical study of fluid particle suspension flowing in an accelerated porous channel under unsteady hydromagnetic Couette flow was investigated by Jha and Malgwi [41]. Dou [42] investigate concentric rotating cylinders with stability of Taylor-Couette flow. Deng et al. [43] studied Couette flow with vertical dissipation for a 2D Boussinesq system. Masmoudi et al. [44] investigate a 2D Boussinesq system and the stability of the Couette flow without thermal diffusivity
The main objective of the present study is to investigate the combined effects of chemical

reaction, variable magnetic field and incorporating with the Soret and Dufour effects on unsteady hydromagnetic surface driven flow between two parallel vertical porous plates which should improve the applicability of the studies published in the literature.

2 Mathematical formulation of the problem

Consider the two-dimensional unsteady laminar flow of electrically conducting, incompressible and viscous between two infinite parallel porous vertical plates with constant injection/suction velocity $u = u_o$, variable magnetic field strength vector ($\vec{B} = (B_0, B_y)$) and a constant magnetic field B_0 applied normal to the plate as shown in Figure 1 . The fluid flow between two parallel vertical porous plates at $x = 0$ and $x = h$ of infinite length. Both the plates at $x = 0$ and $x = h$ and the fluid are initially stationary at concentration $C = C_{sp}$ and temperature $T = T_{sp}$ at time $t \leq 0$. When $t > 0$, the porous plate at $x = 0$ starts moving in its own plane with impulsive motion with velocity U and its concentration and temperature rises to $T = T_{mp}$ and $C = C_{mp}$ respectively while the other porous plate at a distance h from it is fixed and maintained the concentration $C = C_{sp}$ and temperature $T = T_{sp}(T_{mp} > T_{sp})$. Since the porous plates are of infinite length, the concentration, velocity, induced magnetic profile and temperature are functions of x and t. The fluid is injected and sucked with the constant velocity u_o. The unsteady flow is governed by the

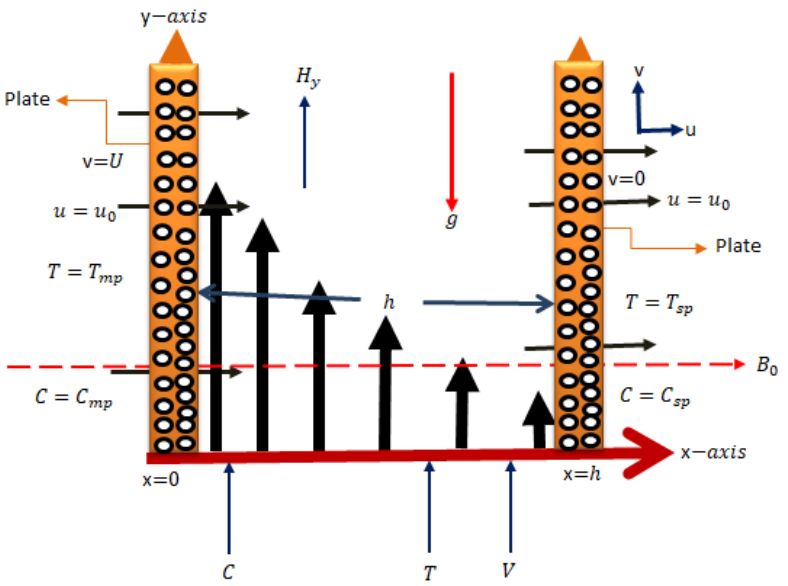

Figure 1: Schematic diagram of the physical system.

following partial differential equations. Using Boussinesq's approximation, the governing equations for the present physical system in dimensional form are as follow:-
Continuity equation .

$$\frac{\partial u}{\partial x} = 0 \tag{1}$$

Momentum equation

$$\frac{\partial v}{\partial t}+u_0\frac{\partial v}{\partial x}=\frac{\mu}{\rho k_p}v+\nu\frac{\partial^2 v}{\partial x^2}+\beta_*^t g(T-T_{sp})+ \\ \beta_*^c g(C-C_{sp})-\frac{\sigma(u_o H_0\mu_e^2 H_y-v\mu_e^2 H_0^2)}{\rho} \tag{2}$$

Energy Equation.

$$\left[\frac{\partial T}{\partial t}+u_0\frac{\partial T}{\partial x}\right]=\frac{k}{\rho C_p}\left[\frac{\partial^2 T}{\partial x^2}\right]+\frac{\mu}{\rho C_p}\left(\frac{\partial v}{\partial x}\right)^2+\frac{K_t D_m}{C_p C_s}\frac{\partial^2 C}{\partial x^2} \tag{3}$$

Concentration equation.

$$\frac{\partial C}{\partial t}=-u_0\frac{\partial C}{\partial x}+D_m\frac{\partial^2 C}{\partial x^2}-k_r(C-C_{sp})+\frac{D_m K_t}{T_m}\frac{\partial^2 T}{\partial x^2} \tag{4}$$

Magnetic induction equation.

$$\frac{\partial H_y}{\partial t}=-u_0\frac{\partial H_y}{\partial x}+H_0\frac{\partial v}{\partial x}+\frac{1}{\mu_e\sigma}\frac{\partial^2 H_y}{\partial x^2}. \tag{5}$$

The corresponding initial and boundary conditions are:-

$$t>0:\begin{cases} v=U, T=T_{mp}, C=C_{mp}, & H_y=H_0 \text{ at } \quad x=0 \\ v=0, T=T_{sp}, C=C_{sp}, & H_y=0 \quad \text{at} \quad x=h \end{cases} \\ t\le 0: v=0, T=T_{sp}, \quad C=C_{sp}, H_y=0 \quad \text{for } 0\le x\le h \tag{6}$$

To non-dimensionalize the governing equations, We use the following dimensionless quantities for the present hydromagnetic problem

$$H_y=H^*H_0, v^*=\frac{v}{U}, \quad t^*=\frac{\nu t}{h^2}, x^*=\frac{x}{h}, M=\frac{H_0^2\sigma\mu_e^2h^2}{\nu\rho}, \\ S=\frac{u_0h}{\nu}, X=\frac{h^2}{k_p}, Re=\frac{uh}{\nu}, Ec=\frac{u^2}{c_p(T_{mp}-T_{sp})}, \theta=\frac{T-T_{sp}}{T_{mp}-T_{sp}}, \\ \phi=\frac{C-C_{sp}}{C_{mp}-C_{sp}}, Gr=\frac{g\beta_*^t(T_{mp}-T_{sp})h^2}{\nu U}, Gc=\frac{g\beta_*^c(C_{mp}-C_{sp})h^2}{\nu U} \\ R=\frac{k_rh^2}{\nu}, Sc=\frac{\nu}{D}, \quad Pr=\frac{\mu c_p\nu}{k}, Sr=\frac{D_mK_t(T_{mp}-T_{sp})}{T_m(C_{mp}-C_{sp})\nu} \\ Df=\frac{K_tD_m(C_{mp}-C_{sp})}{\nu C_pC_s(T_{mp}-T_{sp})}, Pr_m=\frac{Rm}{Re}=\mu_e\sigma\nu, \tag{7}$$

By using the dimensionless quantities defined in Eq.(7); Eqs.(2), (3), (4) and (5) in non-dimensional form are:

$$\frac{\partial v^*}{\partial t^*}+S\frac{\partial v^*}{\partial x^*}=Xv^*+\frac{\partial^2 v^*}{\partial x^{*2}}+Gr\theta+Gc\phi-M\left(SH^*-v^*\right). \tag{8}$$

$$\frac{\partial\theta}{\partial t^*}+S\frac{\partial\theta}{\partial x^*}=\frac{1}{Pr}\left[\frac{\partial^2\theta}{\partial x^{*^2}}\right]+Ec\left(\frac{\partial v^*}{\partial x^*}\right)^2+Df\frac{\partial^2\phi}{\partial x^{*^2}} \tag{9}$$

$$\frac{\partial\phi}{\partial t^*}=-S\frac{\partial\phi}{\partial x^*}+\frac{1}{Sc}\frac{\partial^2\phi}{\partial x^{*^2}}-R\phi+Sr\frac{\partial^2\theta}{\partial x^{*^2}} \tag{10}$$

$$\frac{\partial H^*}{\partial t^*}=-S\frac{\partial H^*}{\partial x^*}+\frac{1}{Re}\frac{\partial v^*}{\partial x^*}+\frac{Re}{Rm}\frac{\partial^2 H^*}{\partial x^{*^2}} \tag{11}$$

The corresponding initial and boundary conditions are:-

$$t>0:\begin{cases}v^*=1,\theta=1,\phi=1 \quad H^*=1 \quad \text{at} \quad x^*=0\\ v^*=0,\theta=1,\phi=1 \quad H^*=0 \quad \text{at} \quad x^*=1\end{cases}$$
$$t\le 0: v^*=0,\theta=1,\phi=1,H^*=0 \quad \text{for} \quad 0\le x^*\le 1 \tag{12}$$

3 Numerical solution procedure

The nonlinear partial differential equations of momentum, concentration, energy and induced given in (8), (9), (10) and (11) are solved by explicit finite difference method subject to the initial and boundary condition (12). In difference form the governing equations becomes

The equation of motion is given by

$$v_j^{k+1}=v_j^k-\Delta tS\left[\frac{v_{j+1}^k-v_{j-1}^k}{2\Delta x}\right]+Xv_j^k\Delta t+\Delta t\left(\frac{v_{j+1}^k-2v_j^k+v_{j-1}^k}{(\Delta x)^2}\right)$$
$$+GrT_j^k\Delta t+GcC_j^k\Delta t-M(SH_j^k-v_j^k)\Delta t \tag{13}$$

The equation of energy is given by

$$T_j^{k+1}=T_j^k-S\Delta t\left(\frac{T_{j+1}^k-T_{j-1}^k}{2\Delta x}\right)+\frac{\Delta t}{Pr}\left(\frac{T_{j+1}^k-2T_j^k+T_{j-1}^k}{(\Delta x)^2}\right)$$
$$+Ec\Delta t\left[\frac{v_{j+1}^k-v_{j-1}^k}{2\Delta x}\right]^2+Df\Delta t\left[\frac{C_{j+1}^k-2C_j^k+C_{j-1}^k}{(\Delta x)^2}\right] \tag{14}$$

Concentration equation is given by

$$C_j^{k+1}=C_j^k-S\Delta t\left[\frac{C_{j+1}^k-C_{j-1}^k}{2\Delta x}\right]+\frac{\Delta t}{Sc}\left[\frac{C_{j+1}^k-2C_j^k+C_{j-1}^k}{(\Delta x)^2}\right]$$
$$-R\Delta tC_j^k+\Delta tSr\left[\frac{T_{j+1}^k-2T_j^k+T_{j-1}^k}{(\Delta x)^2}\right] \tag{15}$$

Equation of induced magnetic field profile is given by

$$H_j^{k+1}=H_j^k-S\Delta t\left[\frac{H_{j+1}^k-H_{j-1}^k}{2\Delta x}\right]+\frac{\Delta t}{Re}\left[\frac{v_{j+1}^k-v_{j-1}^k}{2\Delta x}\right]+$$
$$\frac{Re\Delta t}{Rm}\left[\frac{H_{j+1}^k-2H_j^k+H_{j-1}^k}{(\Delta x)^2}\right] \tag{16}$$

with the following initial and boundary conditions

$$t > 0 : \begin{cases} v(j,k) = 1, T(j,k) = 1, C(j,k) = 1 \quad H(j,k) = 1 \quad \text{at } x = 0 \\ v(j,k) = 0, T(j,k) = 0, C(j,k) = 0 \quad H(j,k) = 0 \quad \text{at } x = 1 \end{cases} \tag{17}$$
$$t \leq 0 : v(j,k) = 0, T(j,k) = 0, C(j,k) = 0, H(j,k) = 0 \text{ for } 0 \leq x \leq 1$$

3.1 Other important physical parameters

For practical engineering design and application, the quantities of interest are Sherwood number (Sh), Nusselt number (Nu) and Skin Friction coefficient. The Sherwood number at the moving plate is given by

$$Sh = \frac{x' q_m}{C_{mp} - C_{sp}} \tag{18}$$

where by $q_m = -\left(\frac{\partial C}{\partial x}\right)_{y=0,1}$

Using (7) becomes

$$ShRe_x^{-1} = -\left(\frac{\partial \phi}{\partial x^*}\right)_{y^*=0,1} \tag{19}$$

The Nusselt number (Nu) at the moving plate is given by

$$Nu = \frac{x' q_h}{T_{mp} - T_{sp}} \tag{20}$$

where by $q_h = -\left(\frac{\partial T}{\partial x}\right)_{y=0,1}$

Using (7) becomes

$$NuRe_x^{-1} = -\left(\frac{\partial \theta}{\partial x^*}\right)_{y^*=0,1} \tag{21}$$

The Skin friction at the moving plate is given by.

$$C_f = \frac{x' \tau_w}{\rho U \nu} \tag{22}$$

where by $\tau_w = \mu \left(\frac{\partial v}{\partial x}\right)_{y=0,1}$

Using (7) becomes

$$C_f = \left(\frac{\partial v^*}{\partial x^*}\right)_{y^*=0,1} \tag{23}$$

4 Results and discussion

The numerical solution of temperature, velocity, concentration and induced magnetic field profiles using numerical approximation finite difference method is performed with the aid of non-dimensional parameters that govern the flow problem. To study the effects of various

flow parameters like Reynold's number, magnetic Reynold's number, Prandtl number, Grashof numbers for heat and mass transfer, Schmidt number, Eckert number, magnetic parameter, Dufour number, Soret number, suction/injection parameter and permeability parameter were varied to investigate how they affect the flow variables.

4.1 The effects of varying Grashof number for heat transfer (Gr) on Velocity profiles

From Figure 2, it's observed that an increase Grashof number for heat transfer (Gr) leads to an increase in the velocity profiles . Since Grashof number for heat transfer is represented by ratio of the thermal buoyancy force to the viscous force. Increasing the Grashof number reduce the viscous force and increase thermal buoyancy force thus leads to an increase in the velocity of the fluid.

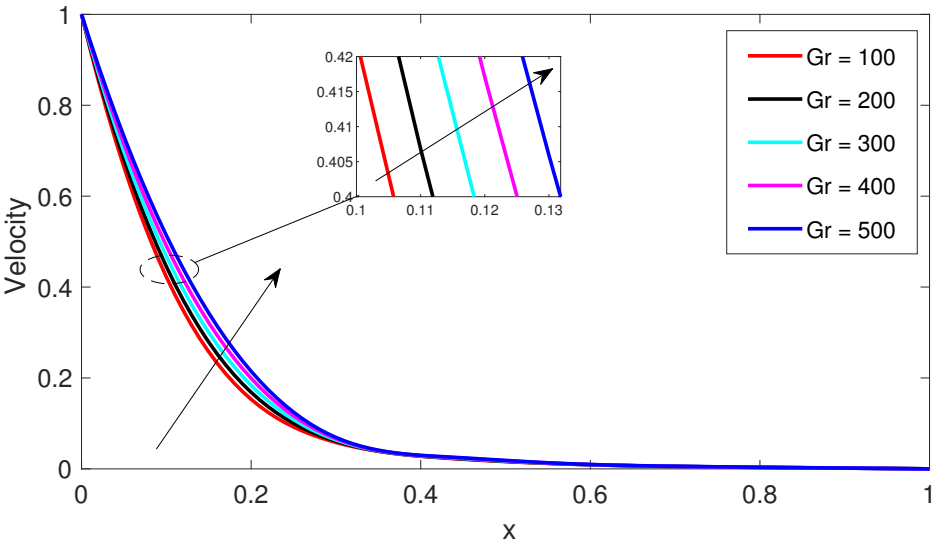

Figure 2: Velocity profiles for different values of Gr

4.2 The effects of varying Grashof number for mass transfer (Gc) on velocity profiles

From Figure 3, it is observed that the velocity of the fluid increases with an increase in the Grashof number for mass transfer(Gc). Since Grashof number for mass transfer is represented by ratio of the species buoyancy force to the viscous force. Increasing Grashof number leads to decrease in the viscosity of the fluid which results to decrease in the viscous force which leads to an increase in the species bouyance force and hence increase the velocity profiles.

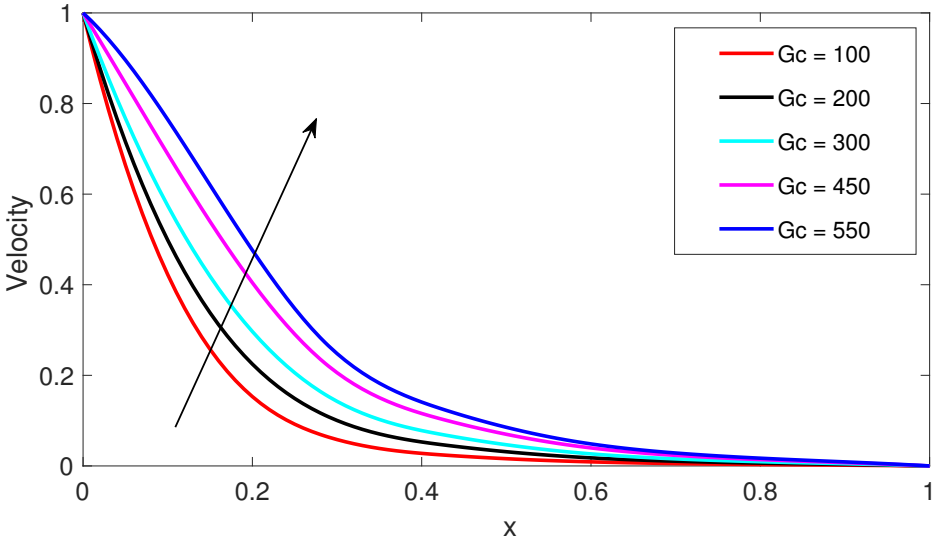

Figure 3: Velocity profiles for different values of Gc

4.3 The effects of varying magnetic parameter (M) on velocity profiles

From Figure 4 , it is observed that increase in the magnetic parameter leads to a decrease in the velocity profiles. Since magnetic parameter is ratio of electromagnetic force to an inertia force, then increasing magnetic parameter leads to an increase in electromagnetic force which caused by magnetic field that control the fluid flow characteristics. The presence of a magnetic field in an electrically conducting fluid enhance the Lorentz force which acts against to the fluid flow when magnetic field is applied normal to the direction of the fluid flow and thus decrease the velocity profiles

4.4 The effects of varying permeability parameter (X) on velocity profiles

From Figure 5, it is observed that increase in the permeability parameter(X) leads to an increase in the velocity profiles. Increasing the permeability parameter leads to decrease in the acceleration of the fluid flow. The velocity distribution of porous medium resistance can be neglected when there is very large holes of the medium and thus the fluid velocity increase.

4.5 The effects of varying suction/injection (S) on velocity profiles

From Figure 6, it is observed that increase in suction parameter leads to an increase in the velocity of the fluid. Suction results in the thinning of the momentum boundary layer of the fluid flow, decrease in pressure which leads to increase the velocities. It is noted that fluid velocity increases with increasing injection parameter. The Injection

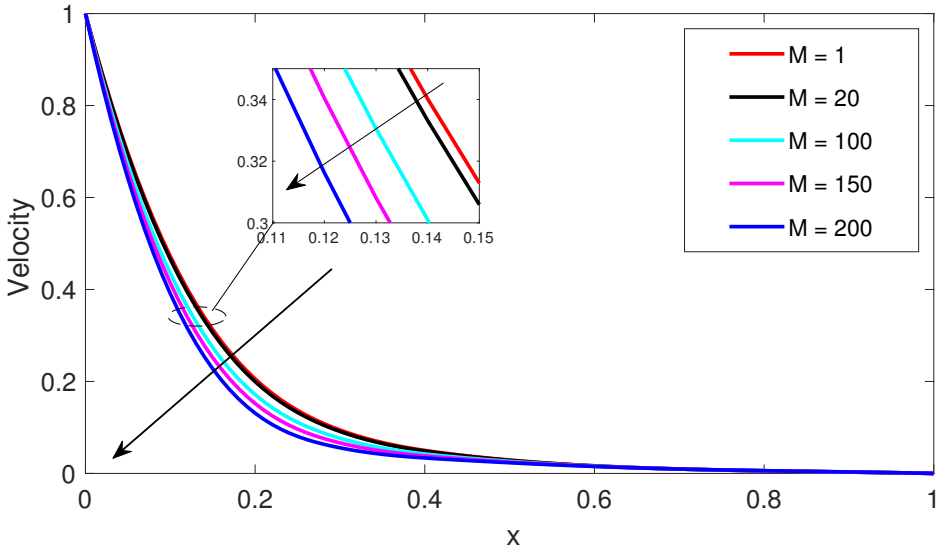

Figure 4: Velocity profiles for different values of M

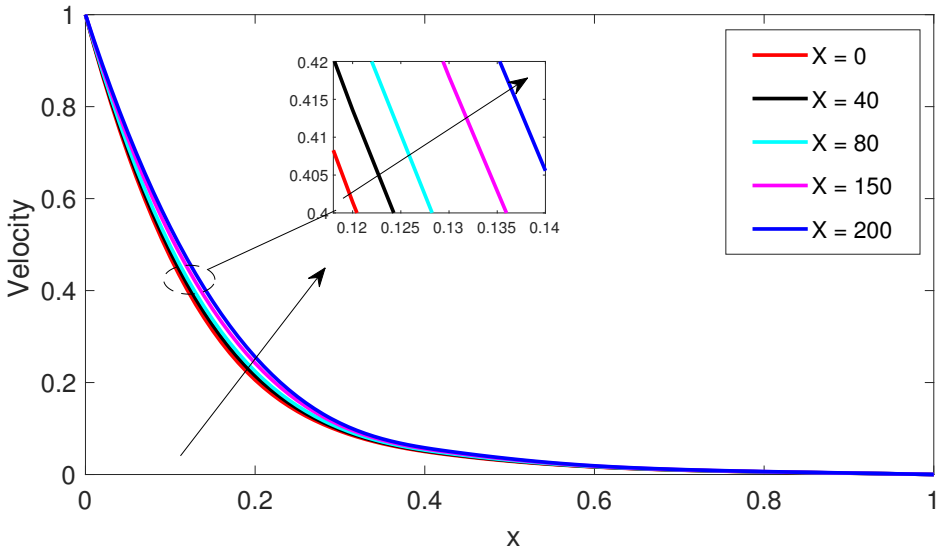

Figure 5: Velocity profiles for different values of X

parameter increases with increasing the injection velocity v_0 and Lorentz force is increased by increasing the injection velocity. Since the Lorentz force acts in the same direction of the injection velocity, therefore increasing injection parameter leads to an increase in the Lorentz force, and hence an increase in the velocity profiles.

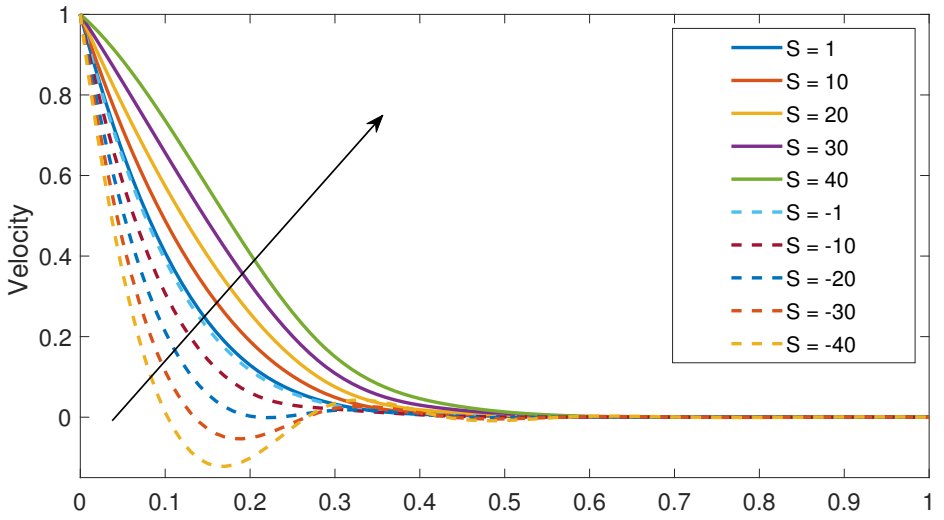

Figure 6: Velocity profiles for different values of S

4.6 The effects of varying Dufour number(Df) on velocity profiles

From Figure 7, it is observed that increase in the Dufour number(Df) leads to increase in the velocity of the fluid. The Dufour number is the energy flux(thermal flux) caused by mass concentration gradient. The Dufour number signifies the contribution of the concentration gradients to the thermal energy flux in the flow. From the definition of the Dufour number, an increase in Df translates directly to a decrease in the temperature profiles of the fluid, or to an increase in the concentration profiles of the fluid which lead to an increase the velocity profiles.

4.7 The effects of varying Soret number(Sr) on velocity profiles

From Figure 8, it is observed that increase in the Soret number(Sr) leads to an increase in the velocity of the fluid. The Soret number signifies the contribution of the temperature gradients to the mass flux in the flow. From the definition of the Soret number, an increase in Sr translates directly to a decrease in the concentration profiles of the fluid, or to an increase in the temperature profiles of the fluid and resulted to an increase in the velocity of the fluid.

4.8 The effects of varying Schmidt number(Sc) on velocity profiles

From Figure 9, it is observed that increase in the Schmidt number(Sc) leads to a decrease in the velocity of the fluid. Increasing the Schmidt number reduces the mass diffusivity, which leads to a decrease in the fluid velocity due to an increase of the viscous drag on the fluid.

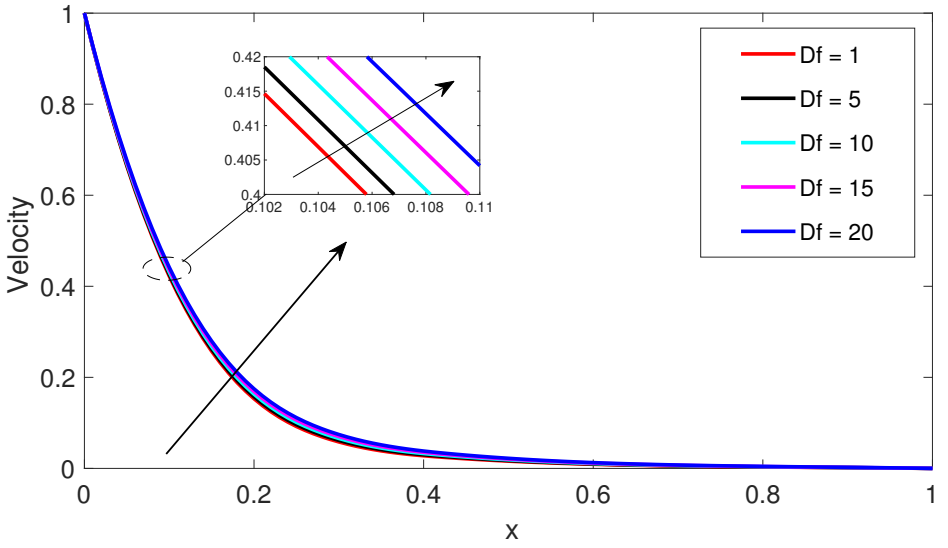

Figure 7: Velocity profiles for different values of Df

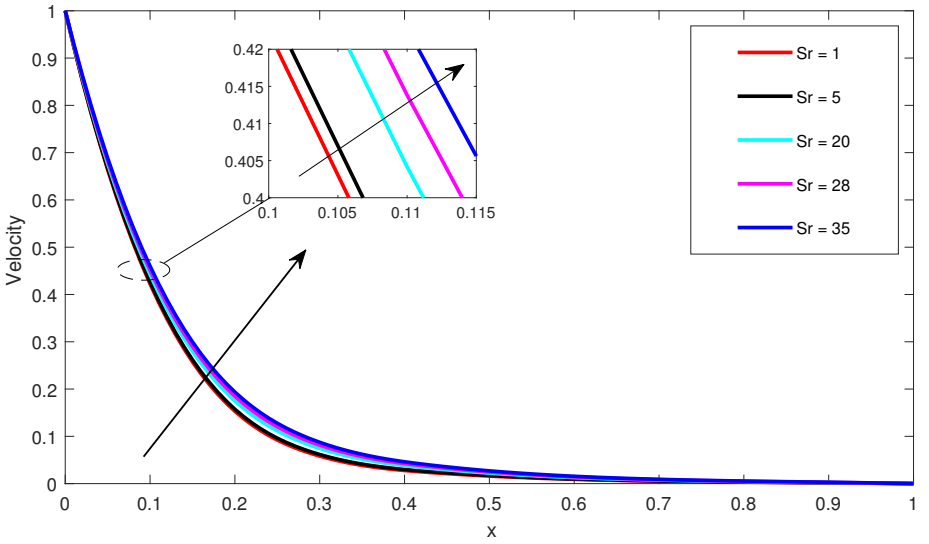

Figure 8: Velocity profiles for different values of Sr

4.9 The effects of varying Prandtl number(Pr) on velocity profiles

From Figure 10, it is observed that increase in the Prandtl number(Pr) leads to a decrease in the velocity of the fluid. Increasing the Prandtl number reduces the thermal diffusivity which leads to increase the viscosity of the fluid and thus decrease the velocity of the fluid.

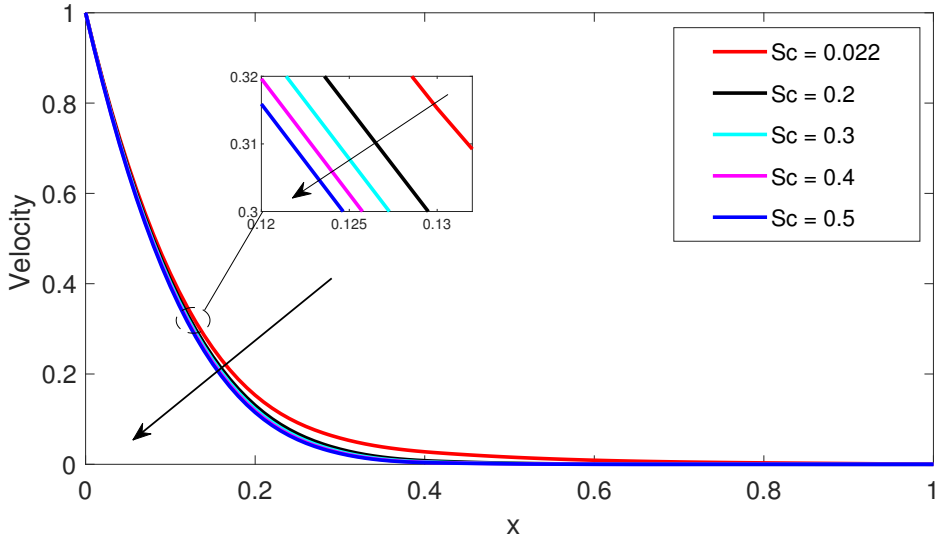

Figure 9: Velocity profiles for different values of Sc

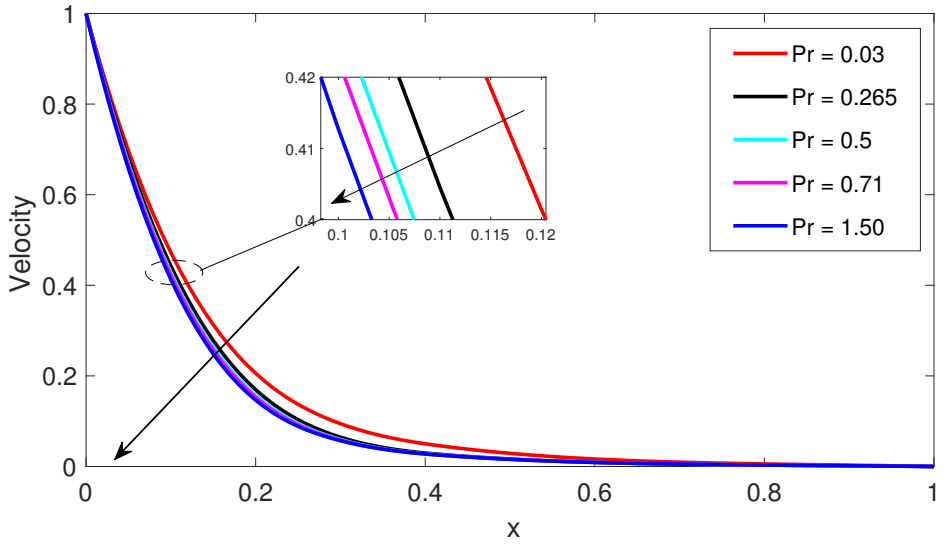

Figure 10: Velocity profiles for different values of Pr

4.10 The effects of varying chemical reaction parameter (R) on concentration profiles

From Figure 11, it is observed that increase in the chemical reaction parameter (R) leads to a decrease in the fluid concentration. This is caused by the negative chemical reaction reduces or decreases the concentration boundary layer thickness and increases the mass transfer.

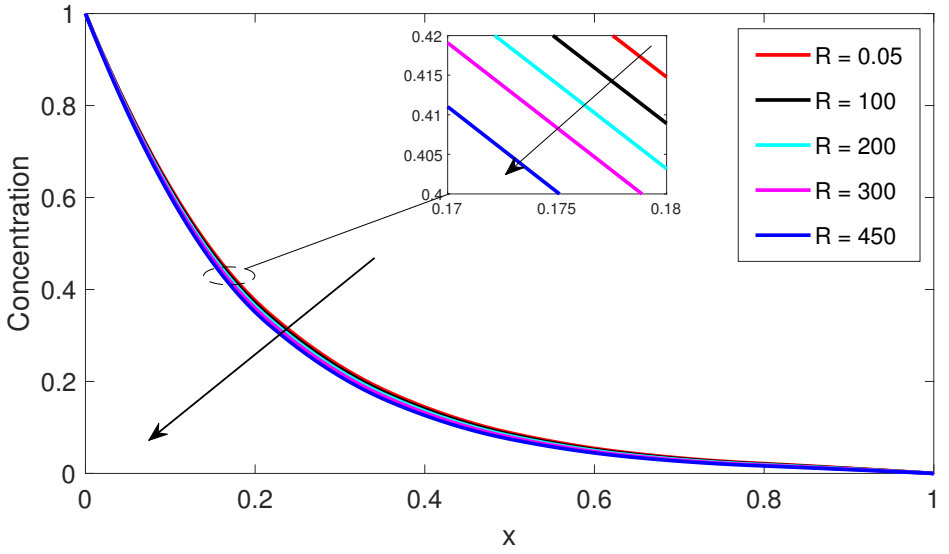

Figure 11: Concentration profiles for different values of R

4.11 The effects of varying Soret number (Sr) on concentration profiles

From Figure 12, it is observed that increase in the Soret number (Sr) leads to an increase in the concentration of the fluid. Soret number is the mass flux caused by temperature gradient. Increasing Soret number cause the concentration of the fluid to decay from the moving plate to the free stream value.

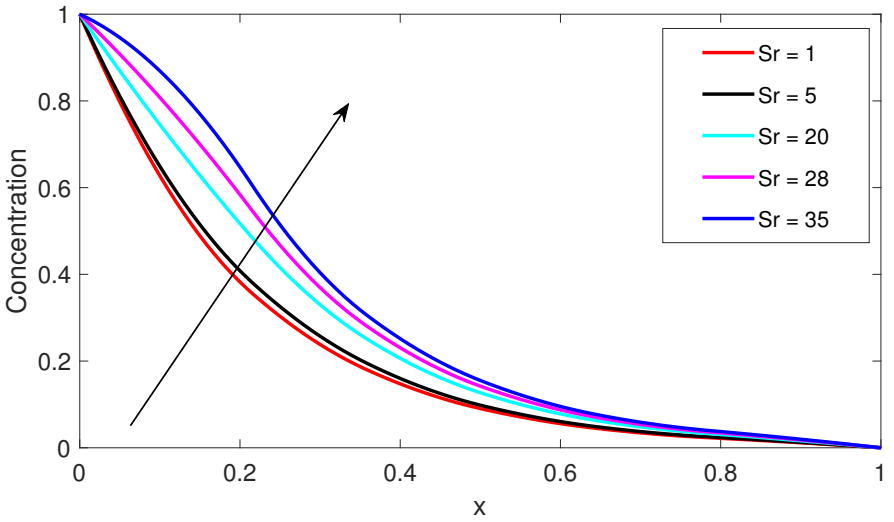

Figure 12: Concentration profiles for different values of Sr

4.12 The effects of varying suction/injection(S) on concentration profiles

From Figure 13, it is observed that increase in the suction (S) leads to a increase in the concentration profiles. Suction results in the thinning of the concentration boundary layer of the fluid flow which leads to increase the concentration profiles. It is noted that concentration profiles increases with increasing injection parameter. Therefore increasing injection parameter leads to an increase in the Lorentz force, and hence an increase in the concentration profiles.

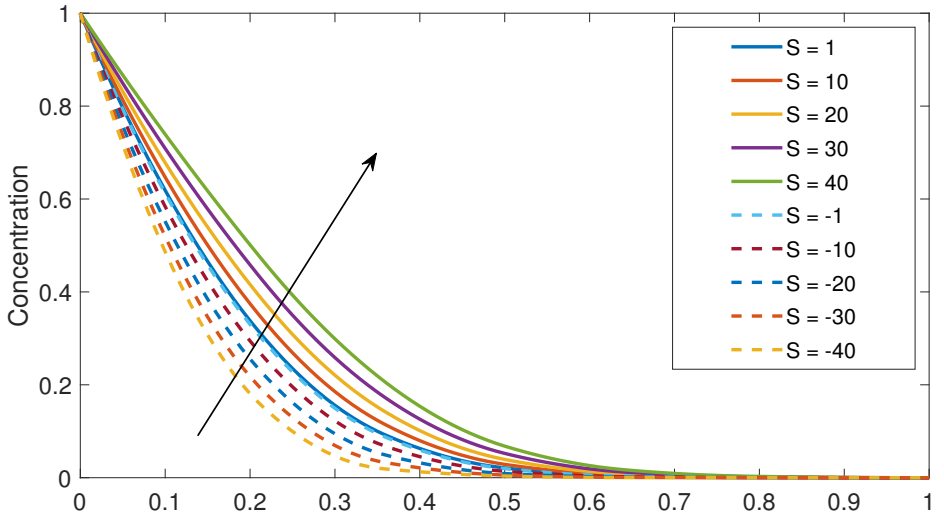

Figure 13: Concentration profiles for different values of S

4.13 The effects of varying Schmidt number(Sc) on concentration Profiles

From Figure 14, it is observed that the concentration of the fluid decreases as the Schmidt number(Sc) increase. Since Schmidt number is the ratio of kinematic air viscosity to the mass diffusivity. Increasing Schmidt number reduces the mass diffusivity, which results in decrease in the concentration of the fluid.

4.14 The effects of varying Reynolds magnetic number(Rm) on induced magnetic field profiles

From Figure 15, it is observed that increase in the Reynolds magnetic number (Rm) leads to a decrease in the induced magnetic field. Increasing the Reynolds magnetic number reduces the magnetic diffusivity, which leads to a decrease in the induced magnetic field by the motion of a conducting medium and thus the induced magnetic field are then advected with the fluid flow

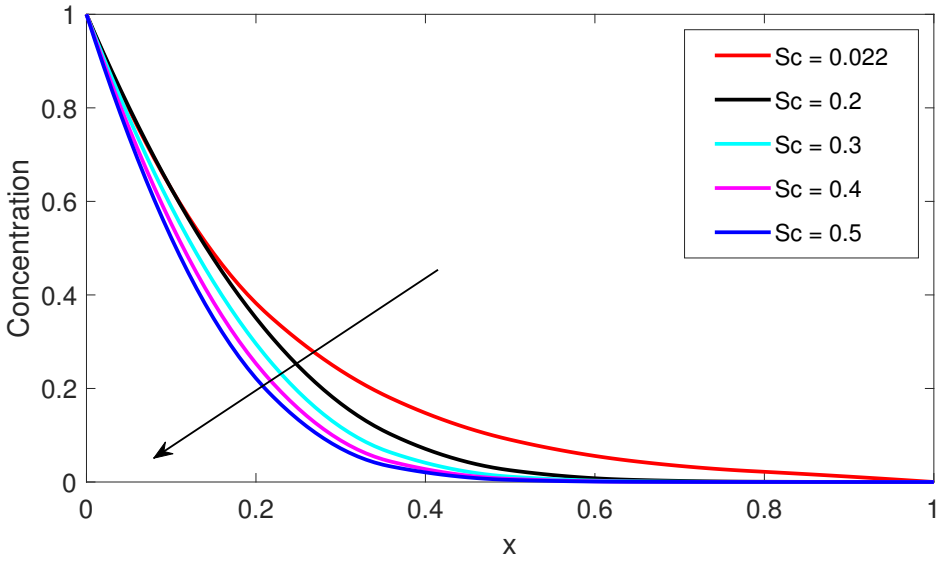

Figure 14: Concentration profiles for different values of Sc

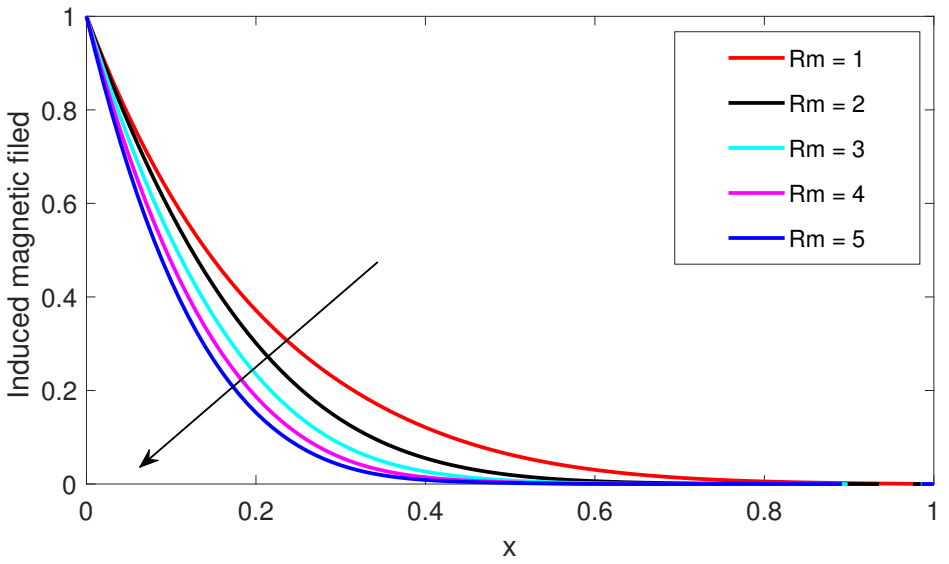

Figure 15: Induced magnetic field profiles for different values of Rm

4.15 The effects of varying suction/injection parameter(S) on induced magnetic profiles

From Figure 16, it is observed that increase in the suction parameter(S) leads to an increase in the induced magnetic field. With an increase in the suction parameter leads to an increase in the velocity of the fluid hence an interaction of fluid and magnetic field increase, hence resulted to an increase in the induced magnetic field. The magnetic induction increase with the increase in the injection parameter. It is observed that increasing

injection parameter leads to an increase in the induced magnetic field. The injection parameter is increased, the velocity of the fluid increased hence leads to an increase in the rate of interaction between the fluid and the magnetic field which leads to an increase in the induced magnetic field.

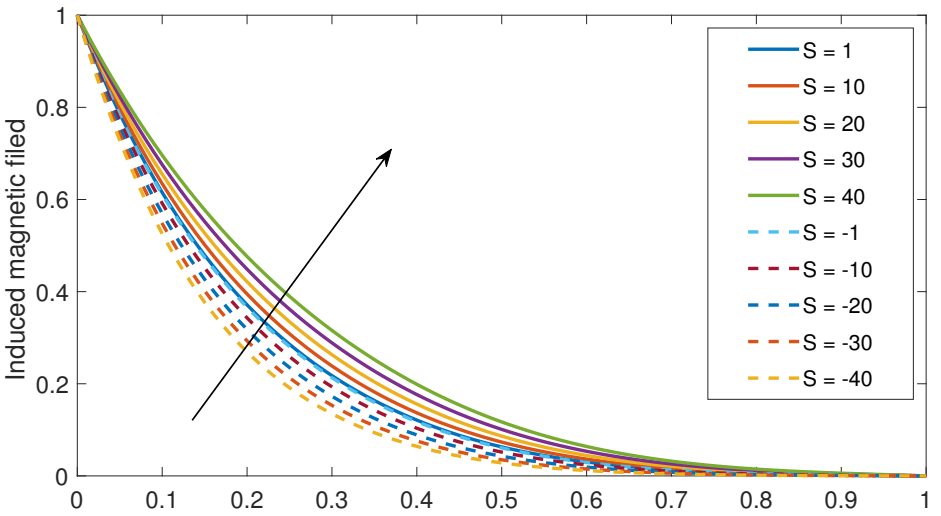

Figure 16: Induced magnetic field profiles for different values of S

4.16 The effects of varying Reynolds number(Re) on induced magnetic field profiles

From Figure 17, it is observed that increase in the Reynolds number(Re) leads to an increase in the induced magnetic field. Since, Reynolds number is the ratio of inertia force to the viscous force. Increasing the Reynolds number reduces the viscous force which leads to an increase of interaction between the fluid and magnetic field and thus an increase of induced magnetic field.

4.17 The effects of varying Dufour number (Df) on temperature profiles

From Figure 18, it is observed that increase Dufour number (Df) leads to an increase in the temperature profiles. The Dufour number is the energy flux(thermal flux) caused by mass concentration gradient. The Dufour number signifies the contribution of the concentration gradients to the thermal energy flux in the flow. From the definition of the Dufour number, an increase in Df translates directly to a decrease in the temperature profiles of the fluid, or to an increase in the concentration profiles of the fluid.

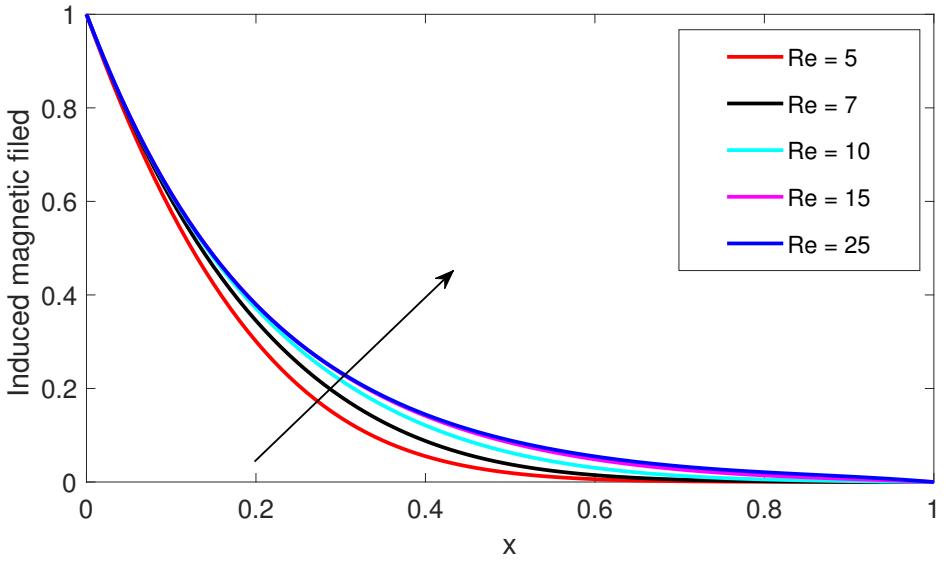

Figure 17: Induced magnetic field profiles for different values of Re

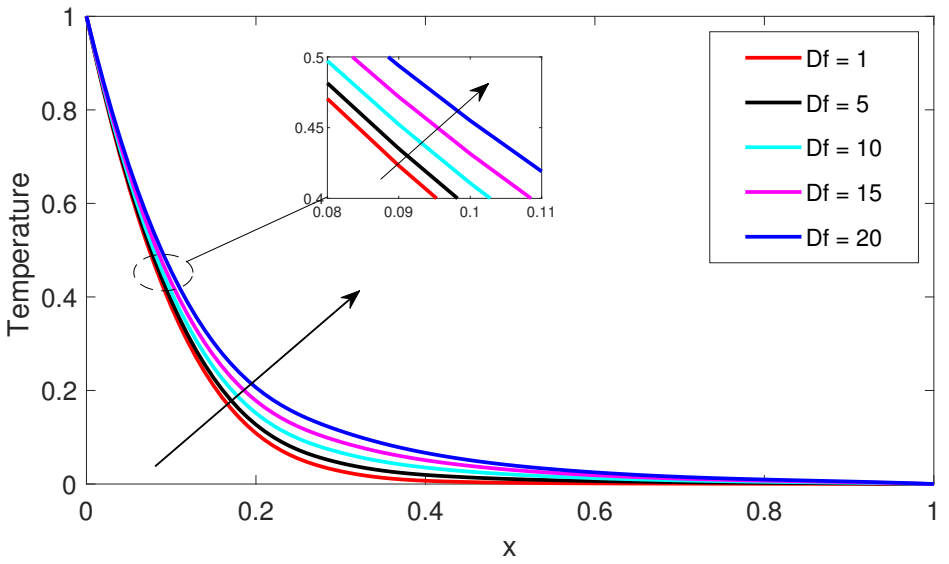

Figure 18: Temperature profiles for different values of Df

4.18 The effects of varying suction/injection parameter (S) on temperature profiles

From Figure 19, it is observed that increase in the suction parameter (S) leads to an increase in the fluid temperature. This is due to the increase in the velocities as a result of the suction which leads to an increase in the kinetic energy which is converted into thermal energy hence the increase in temperature. The temperature increase with the increase in the injection parameter. Injection parameter leads to an increase in the velocities, the

conversion of kinetic energy into thermal energy is also increased hence resulted to an increase in the temperature of the fluid.

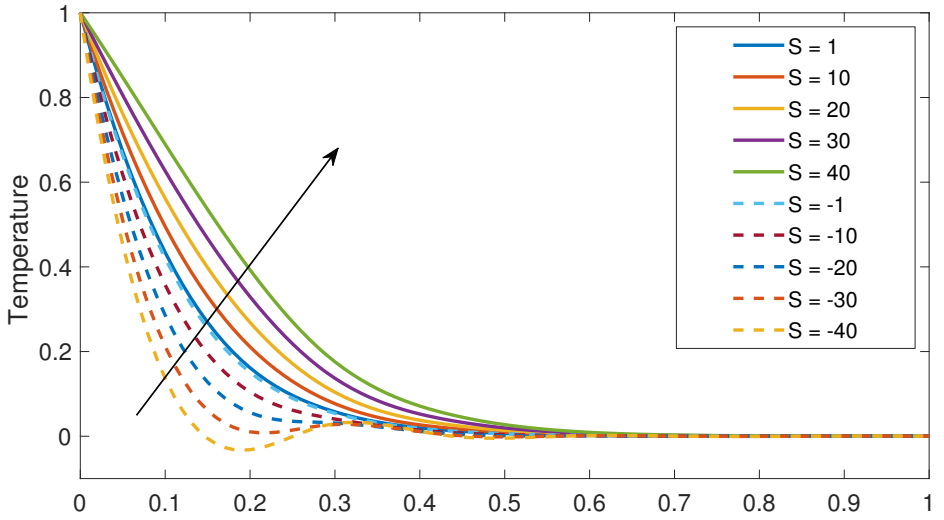

Figure 19: Temperature profiles for different values of S

4.19 The effects of varying Eckert number(Ec) on temperature Profiles

From Figure 20, it is observed increase in the Eckert number(Ec) leads to an increase in the temperature profile. Since, Eckert number is the ratio of the fluid flow kinetic energy to the enthalpy of the fluid. Increasing Eckert number reduces the enthalpy of the fluid and thus the fluid temperature increases. The motion of the fluid increases as an increase of Eckert number which transform into kinetic energy which lead to an increase of the temparature of the fluid.

4.20 The effects of varying Prandtl number(Pr) on temperature profiles

From Figure 21, it is observed that the temperature of the fluid decrease as the values of the Prandtl number(Pr) increase. Since Prandtl number is the ratio of viscous force/ momentum diffusivity to the thermal diffusivity. Increasing the Prandtl number reduces the thermal diffusivity and increase viscosity of the fluid which leads to an increase of temperature of the fluid which make the fluid to thick and thus move slowly.

4.21 The effects of varying Schmidt number(Sc) on temperature profiles

From Figure 22, it is observed that increase in the Schmidt number(Sc) leads to an increase in the temperature profiles. Schmidt number is the ratio of kinematic air viscosity to the

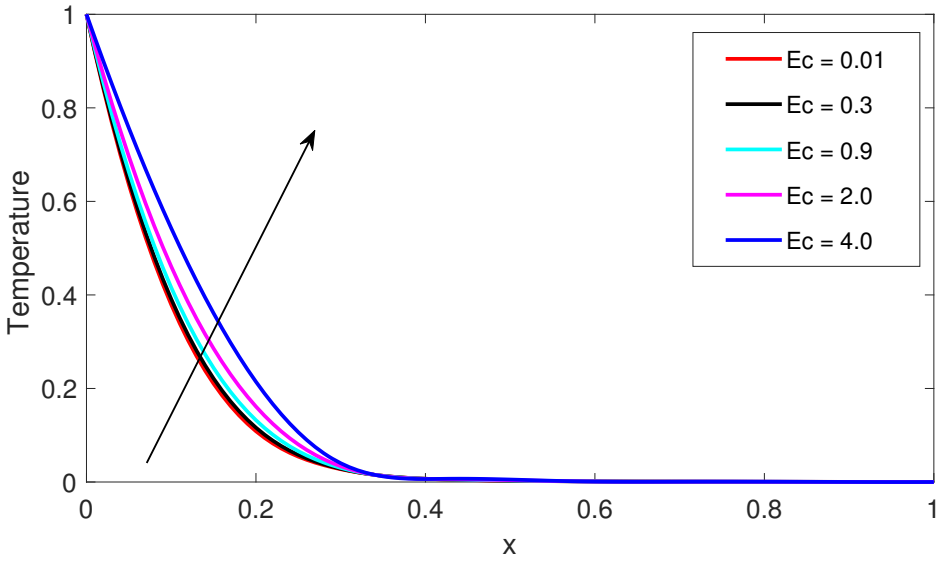

Figure 20: Temperature profiles for different values of Ec

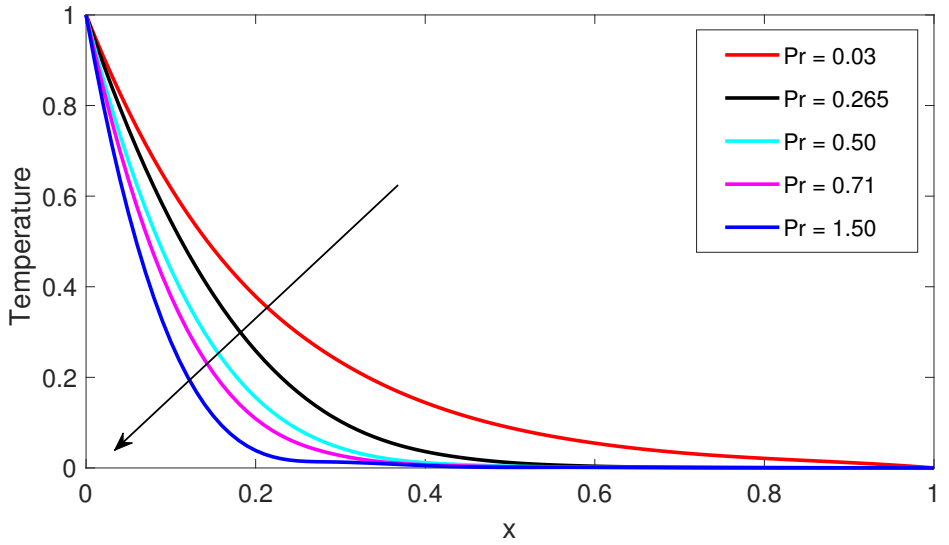

Figure 21: Temperature profiles for different values of Pr

mass diffusivity. Increasing the Schmidt number reduced the mass diffusivity, which leads to increase in the viscosity of the fluid and thus an increase in the temperature of the fluid.

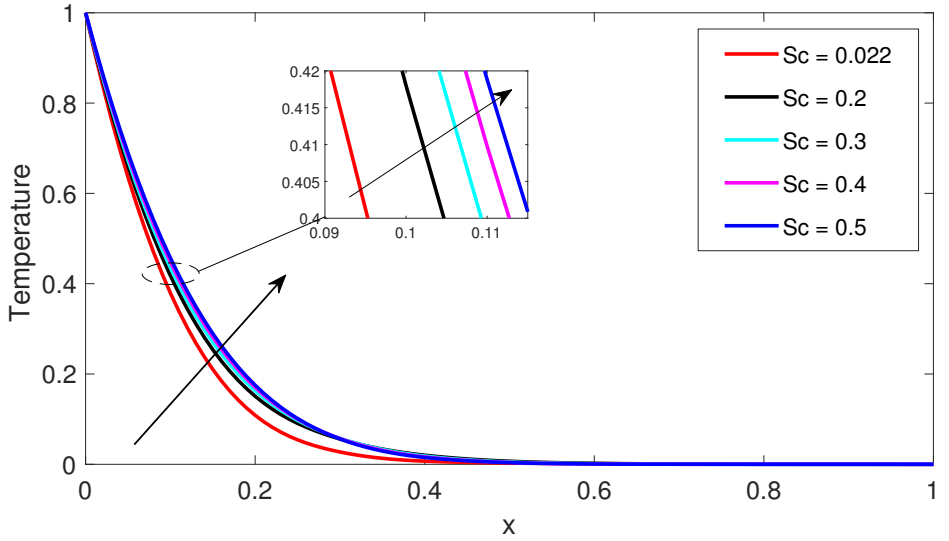

Figure 22: Temperature profiles for different values of Sc

4.22 The effects of varying Soret number(Sr) on temperature profiles

From Figure 23, it is observed that increase in the Soret number(Sr) leads to an increase in the temperature of the fluid. The Soret number signifies the contribution of the temperature gradients to the mass flux in the flow. From the definition of the Soret number, an increase in Sr translates directly to a decrease in the concentration profiles of the fluid and resulted to an increase in the mass transfer which leads to a decrease in temperature of fluid.

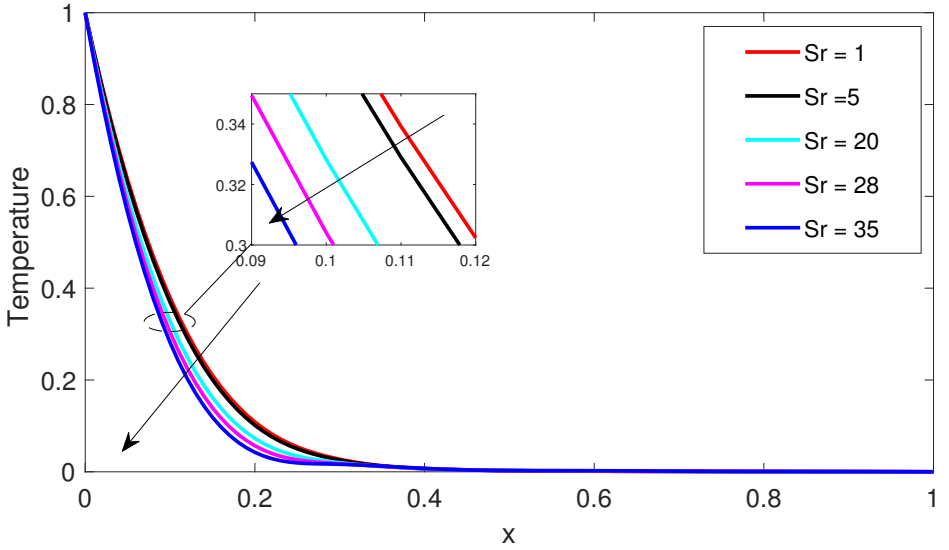

Figure 23: Temperature profiles for different values of Sr

Table 1: Results of Nusselt number for various values of physical parameters.

Pr	M	S	R	Gr	X	Gc	Ec	Sc	Df	Sr	$\theta'(0)$	$\theta'(1)$
0.71	0.2	0.2	0.05	0.1	1	0.1	0.01	0.02	1	1	-0.55937699	-1.59226198
10	0.2	0.2	0.05	0.1	1	0.1	0.01	0.02	1	1	-1.25972941	-0.78391315
0.71	**0.4**	0.2	0.05	0.1	1	0.1	0.01	0.02	1	1	-0.55906145	-1.59226198
0.71	0.2	**1**	0.05	0.1	1	0.1	0.01	0.02	1	1	-0.05055070	-4.89148918
0.71	0.2	0.2	**3**	0.1	1	0.1	0.01	0.02	1	1	0.72543271	-2.05155268
0.71	0.2	0.2	0.05	**1**	1	0.1	0.01	0.02	1	1	-0.55729140	-1.59036017
0.71	0.2	0.2	0.05	0.1	**2**	0.1	0.01	0.02	1	1	-0.56173066	-1.59834925
0.71	0.2	0.2	0.05	0.1	1	**1**	0.01	0.02	1	1	-0.55800128	-1.59105640
0.71	0.4	0.2	0.05	0.1	1	0.1	**0.33**	0.02	1	1	-0.28095737	-2.10084672
0.71	0.2	0.2	0.05	0.1	1	0.1	0.01	**0.22**	1	1	-0.65093761	-1.49311993
0.71	0.2	0.2	0.05	0.1	1	0.1	0.01	0.02	**5**	1	-1.07573701	-0.93828987
0.71	0.2	0.2	0.05	0.1	1	0.1	0.01	0.02	1	**5**	-1.06188904	-0.94251402

From Table 1 shows the effects of Schmidt number, Magnetic parameter, Chemical reaction parameter, Grashof number for heat and mass transfer, Suction/injection parameter, Prandtl number, Dufour number , Eckert number and Permeability parameter on Nusselt number at the stationary and moving plates. It's observed that the Nusselt number $\theta'(1)$ at the stationary plate increases with an increase in Magnetic parameter, Chemical reaction parameter, Grashof number for heat and mass transfer and Suction/injection parameter whereas decrease with an increase in Prandtl number, Dufour number, Soret number, Schmidt number and Permeability parameter. The Nusselt number $\theta'(0)$ at the moving plate increases with an increase in Prandtl number, Dufour number, Soret number, Grashof number for heat and mass transfer and Schmidt number whereas decrease with an increase in Suction/injection parameter, Chemical reaction parameter, Eckert number and Permeability parameter.

From Table 2 shows the effects of Schmidt number, Magnetic parameter, Chemical reaction parameter, Grashof number for heat and mass transfer, Suction/injection parameter, Prandtl number, Dufour number , Eckert number and Permeability parameter on Skin-friction coefficient at the stationary and moving plates. It's observed that the Skin-friction coefficient $V^{*'}(1)$ at the stationary plate increases with an increase in Chemical reaction parameter, Prandtl number, Permeability parameter and Dufour number whereas decrease with an increase in Schmidt number, Magnetic parameter, Grashof number for heat and mass transfer, Suction/injection parameter, Soret number and Eckert number. The Skin-friction coefficient $V^{*'}(0)$ at the moving plate increases with an increase in Schmidt number, Magnetic parameter, Grashof number for heat and mass

Table 2: Results of Skin-friction coefficient for various values of physical parameters.

Pr	M	S	R	Gr	X	Gc	Ec	Sc	Df	Sr	$V^{*'}(0)$	$V^{*'}(1)$
0.71	0.2	0.2	0.05	0.1	1	0.1	0.01	0.022	1	1	-0.84502078	-1.24058896
10	0.2	0.2	0.05	0.1	1	0.1	0.01	0.022	1	1	-0.84498960	-1.24061729
0.71	**0.4**	0.2	0.05	0.1	1	0.1	0.01	0.022	1	1	-0.90796670	-1.21661574
0.71	0.2	**1**	0.05	0.1	1	0.1	0.01	0.022	1	1	-1.57297817	-0.52311441
0.71	0.2	0.2	**3**	0.1	1	0.1	0.01	0.022	1	1	-0.84239937	-1.24255655
0.71	0.2	0.2	0.05	**1**	1	0.1	0.01	0.022	1	1	-1.14716477	-1.05177746
0.71	0.2	0.2	0.05	0.1	**2**	0.1	0.01	0.022	1	1	-0.42420234	-1.72448690
0.71	0.2	0.2	0.05	0.1	1	**1**	0.01	0.022	1	1	-1.08927484	-1.13015022
0.71	0.4	0.2	0.05	0.1	1	0.1	**0.33**	0.022	1	1	-0.84503658	-1.24057412
0.71	0.2	0.2	0.05	0.1	1	0.1	0.01	**0.22**	1	1	-0.84533646	-1.24028371
0.71	0.2	0.2	0.05	0.1	1	0.1	0.01	0.022	**5**	1	-0.84499648	-1.24061112
0.71	0.2	0.2	0.05	0.1	1	0.1	0.01	0.022	1	**5**	-0.84685743	-1.23874778

transfer, Suction/injection parameter, Eckert number and Soret number whereas decrease with an increase in Chemical reaction parameter, Prandtl number, Permeability parameter and Dufour number.

From Table 3 shows the effects of Schmidt number, Magnetic parameter, Chemical reaction parameter, Grashof number for heat and mass transfer, Suction/injection parameter, Prandtl number, Dufour number , Eckert number and Permeability parameter on Sherwood number at the stationary and moving plates. It's observed that the Sherwood number $\phi'(1)$ at the stationary plate increases with an increase in Magnetic parameter, Chemical reaction parameter, Grashof number for heat and mass transfer, Suction/injection parameter and Eckert number whereas decrease with an increase in Schmidt number, Prandtl number, Dufour number, Permeability parameter and Soret number. The Sherwood number $\phi'(0)$ at the moving plate increases with an increase in Schmidt number, Magnetic parameter, Grashof number for heat and mass transfer, Prandtl number, Dufour number and Soret number whereas decrease with an increase in Chemical reaction parameter, Suction/injection parameter, Permeability parameter and Eckert number.

5 Validation of Results

Comparison with previous studies available in the literature has been done and an excellent agreement established. This result agrees with Jha et al. [21] and Raju et al. [27], when there is absence of S, induced magnetic field and X.

Table 3: Results of Sherwood number(Sh) for various values of physical parameters.

Pr	M	S	R	Gr	X	Gc	Ec	Sc	Df	Sr	$\phi'(0)$	$\phi'(1)$
0.71	0.2	0.2	0.05	0.1	1	0.1	0.01	0.022	1	1	1.45005803	0.40481853
10	0.2	0.2	0.05	0.1	1	0.1	0.01	0.022	1	1	0.75383484	1.21155290
0.71	**0.4**	0.2	0.05	0.1	1	0.1	0.01	0.022	1	1	1.45037378	0.40524984
0.71	0.2	**1**	0.05	0.1	1	0.1	0.01	0.022	1	1	1.92491847	-2.88234316
0.71	0.2	0.2	**3**	0.1	1	0.1	0.01	0.022	1	1	3.30872649	-0.19238054
0.71	0.2	0.2	0.05	**1**	1	0.1	0.01	0.022	1	1	1.45214244	0.40715003
0.71	0.2	0.2	0.05	0.1	**2**	0.1	0.01	0.022	1	1	1.44770490	0.39916766
0.71	0.2	0.2	0.05	0.1	1	**1**	0.01	0.022	1	1	1.45143398	0.40645403
0.71	0.4	0.2	0.05	0.1	1	0.1	**0.33**	0.022	1	1	1.72648517	-0.10223968
0.71	0.2	0.2	0.05	0.1	1	0.1	0.01	**0.22**	1	1	1.31467960	0.53864319
0.71	0.2	0.2	0.05	0.1	1	0.1	0.01	0.022	**5**	1	0.93687154	1.05761633
0.71	0.2	0.2	0.05	0.1	1	0.1	0.01	0.022	1	**5**	0.70445453	1.28272175

6 Conclusions

In this study, the problem of an unsteady hydromagnetic surface driven flow between two parallel vertical porous plates in presence of chemical reaction, suction/injection and variable magnetic field has been studied. The governing equations are continuity equation, equation of momentum, energy equation, concentration equation and magnetic induction equation. The objective of this study is to determine the velocity, temperature, concentration and induced magnetic filed profiles. The system of nonlinear PDEs governing the flow were derived, non-dimensionalized and solved numerically by applying numerical approximation finite difference method and implemented in MATLAB. The numerical solutions of the profiles are displayed graphically and discussed. Based on the numerical results it can be concluded that:-

- The fluid velocity increase with the increase in the Grashof number for heat and mass transfer, Permeability parameter (X), suction/Injection parameter (S), Dufour number(Df) and Soret number(Sr) whereas it decrease with the increase in the magnetic parameter(M), Prandtl number (Pr) and Schmidt number (Sc).

- Skin friction coefficient decreases with an increase in Soret number, Dufour number, magnetic permeability and magnetic parameter whereas increase with an increase in suction/injection parameter.

- The fluid concentration decrease with the increase in the chemical reaction parameter (R) and Schmidt number(Sc) whereas it increase with the increase in the suction/injection parameter (S) and Soret number (Sr).

- Nusselt number increases with an increase in Prandtl number, Dufour number and Eckert number whereas decrease with an increase in suction/injection parameter.
- The fluid temperature increase with the increase in the Dufour number (Df), suction/injection parameter (S),Schmidt number (Sc) and Eckert number (Ec) whereas it decrease with the increase in the Prandtl number (Pr) and Soret number (Sr).
- Sherwood number increases with an increase in Soret number, suction/injection parameter and chemical reaction parameter whereas decrease with an increase in Schmidt number.
- Increase in the magnetic Reynold's number(Rm) lead to a decrease an induced magnetic field.
- Increase in Reynold's number (Re) and suction/injection parameter (S) lead to an increase in an induced magnetic field.

The findings are found to be in an excellent agreement.

Conflict of interest

The authors declare no conflict of interest.

Data Availability

The data used to support the findings of this study are available from the corresponding author upon request.

Acknowledgment

The authors would like to thank the African Union Commission and Pan African University Institute for Basic Sciences, Technology and Innovation for supporting this research.

References

[1] Y. Demirel, Nonequilibrium thermodynamics: transport and rate processes in physical, chemical and biological systems, Elsevier, 2007. doi:https://doi.org/10.1016/B978-0-444-53079-0.X5000-7.

[2] V. Soundalgekar, Steady mhd couette flow of an electrically conducting, viscous, incompressible rarefied gas under transverse magnetic field, in: Proc. Natl. Inst. Sci. India, Part A, volume 33, Indian Inst. of Tech., Bombay, 1967.

[3] V. Soundalgekar, Heat transfer in MHD Couette flow between conducting walls in slip-flow regime., Technical Report, Indian Inst. of Tech., Bombay, 1970.

[4] V. Soundalgekar, N. Vighnesam, H. Takhar, Hall and ion-slip effects in mhd couette flow with heat transfer, IEEE Transactions on Plasma Science 7 (1979) 178–182. doi:https://doi.org/10.1109/TPS.1979.4317226.

[5] G. Mandal, K. K. Mandal, Effect of hall current on mhd couette flow between thick arbitrarily conducting plate in a rotating system, Journal of the Physical Society of Japan 52 (1983) 470–477. doi:https://doi.org/10.1143/JPSJ.52.470.

[6] V. Soundalgekar, A. Uplekar, Hall effects in mhd couette flow with heat transfer, IEEE Transactions on Plasma Science 14 (1986) 579–583. doi:https://doi.org/10.1109/TPS.1986.4316600.

[7] G. Bodosa, A. Borkakati, Mhd couette flow with heat transfer between two horizontal plates in the presence of a uniform transverse magnetic field, Theoretical and Applied Mechanics (2003) 1–9. doi:https://doi.org/10.2298/TAM0301001B.

[8] M. Alabraba, A. Warmate, A. Amakiri, J. Amonieah, Heat transfer in magneto-hydrodynamic (mhd) couette flow of a two-component plasma with variable wall temperature, Global journal of pure and applied Sciences 14 (2008) 439–449. doi:https://doi.org/10.4314/gjpas.v14i4.16834.

[9] G. Seth, R. Nandkeolyar, N. Mahto, S. Singh, Mhd couette flow in a rotating system in the presence of an inclined magnetic field, Applied Mathematical Sciences 3 (2009) 2919–2932.

[10] J. Umavathi, I. Liu, J. P. Kumar, Magnetohydrodynamic poiseuille-couette flow and heat transfer in an inclined channel, Journal of Mechanics 26 (2010) 525–532.

[11] H. A. Attia, Unsteady mhd couette flow of a viscoelastic fluid with heat transfer, Kragujevac J. Sci 32 (2010) 5–15.

[12] B. K. Jha, C. A. Apere, Unsteady mhd couette flows in an annuli: The riemann-sum approximation approach, Journal of the Physical Society of Japan 79 (2010) 124403. doi:https://doi.org/10.1143/JPSJ.79.124403.

[13] O. A. Bég, S. Ghosh, M. Narahari, Mathematical modeling of oscillatory mhd couette flow in a rotating highly permeable medium permeated by an oblique magnetic field, Chemical Engineering Communications 198 (2010) 235–254. doi:https://doi.org/10.1080/00986445.2010.500165.

[14] H. A. Attia, M. E. Sayed-Ahmed, Transient mhd couette flow of a casson fluid between parallel plates with heat transfer, Italian Journal of pure and applied Mathematics 27 (2010) 19–38.

[15] H. Attia, A. Al-Kaisy, K. Ewis, et al., Mhd couette flow and heat transfer of a dusty fluid with exponential decaying pressure gradient, Journal of Applied Science and Engineering 14 (2011) 91–96. doi:https://doi.org/10.6180/jase.2011.14.2.01.

[16] S. W. Guo, J. C. Leong, Mhd couette flow in cylindrical porous annulus with perfectly conducting walls, in: Applied Mechanics and Materials, volume 284, Trans Tech Publ, 2013, pp. 829–833. doi:https://doi.org/10.4028/www.scientific.net/AMM.284-287.829.

[17] Z. Barikbin, R. Ellahi, S. Abbasbandy, The ritz-galerkin method for mhd couette flow of non-newtonian fluid (2014). doi:https://www.sid.ir/en/journal/ViewPaper.aspx?id=389767.

[18] L. Sreekala, E. K. Reddy, Steady mhd couette flow of an incompressible viscous fluid through a porous medium between two infinite parallel plates under effect of inclined magnetic field, The International Journal of Engineering and Science (IJES) 3 (2014) 18–37.

[19] K. Joseph, S. Daniel, G. Joseph, Unsteady mhd couette flow between two infinite parallel porous plates in an inclined magnetic field with heat transfer, International Journal of Mathematics and Statistics Invention 2 (2014) 103–110.

[20] S. Mosayebidorcheh, M. Hatami, D. Ganji, T. Mosayebidorcheh, S. Mirmohammadsadeghi, Investigation of transient mhd couette flow and heat transfer of dusty fluid with temperature-dependent oroperties., Journal of Applied Fluid Mechanics 8 (2015). doi:https://doi.org/10.18869/ACADPUB.JAFM.67.223.23949.

[21] B. K. Jha, B. Isah, I. Uwanta, Unsteady mhd free convective couette flow between vertical porous plates with thermal radiation, Journal of King Saud University-Science 27 (2015) 338–348. doi:https://doi.org/10.1016/j.jksus.2015.06.005.

[22] E. R. Onyango, M. N. Kinyanjui, S. M. Uppal, Unsteady hydromagnetic couette flow with magnetic field lines fixed relative to the moving upper plate, American Journal of Applied Mathematics 3 (2015) 206–214. doi:doi:10.11648/j.ajam.20150305.11.

[23] P. Vyas, N. Srivastava, Entropy analysis of generalized mhd couette flow inside a composite duct with asymmetric convective cooling, Arabian Journal for Science and Engineering 40 (2015) 603–614. doi:https://doi.org/10.1007/s13369-014-1562-0.

[24] A. O. Ali, O. D. Makinde, Y. Nkansah-Gyekye, Effect of hall current on unsteady mhd couette flow and heat transfer of nano fluids in a rotating system, Appl. Comput. Math. 4 (2015) 232–244. doi:https://doi.org/10.11648/j.acm.20150404.12.

[25] D. Kiema, W. Manyonge, J. Bitok, R. Adenyah, J. Barasa, On the steady mhd couette flow between two infinite parallel plates in an uniform transverse magnetic field, Journal of Applied Mathematics and Bioinformatics 5 (2015) 87–99.

[26] A. T. Ngiangia, A. Okechukwu, Influence of variable electroconductivity and radiation on mhd couette flow, World Scientific News 47 (2016) 241–253.

[27] R. S. Raju, G. Jithender Reddy, J. A. Rao, M. M. Rashidi, Thermal diffusion and diffusion thermo effects on an unsteady heat and mass transfer magnetohydrodynamic

natural convection couette flow using fem, Journal of computational Design and Engineering 3 (2016) 349–362. doi:https://doi.org/10.1016/j.jcde.2016.06.003.

[28] A. O. Ali, O. D. Makinde, Y. Nkansah-Gyekye, Numerical study of unsteady mhd couette flow and heat transfer of nanofluids in a rotating system with convective cooling, International Journal of Numerical Methods for Heat & Fluid Flow (2016). doi:https://doi.org/10.1108/HFF-10-2014-0316.

[29] V. M. Job, S. R. Gunakala, Unsteady mhd free convection couette flow between two vertical permeable plates in the presence of thermal radiation using galerkin's finite element method, International Journal of Mechanical Engineering 2 (2016) 99–110.

[30] Y. Ali, M. Rana, M. Shoaib, Magnetohydrodynamic three-dimensional couette flow of a maxwell fluid with periodic injection/suction, Mathematical problems in Engineering 2017 (2017). doi:https://doi.org/10.1155/2017/1859693.

[31] M. Kamran, I. Siddique, Mhd couette and poiseuille flow of a third grade fluid, Open J. Math. Anal. 1 (2017) 1–19. doi:https://dx.doi.org/10.30538/psrp-oma2017.0006.

[32] M. Kimathi, M. Kinyanjui, E. Onyango, Effects of the direction of a transverse magnetic field on unsteady mhd couette flow with suction and injection (2015).

[33] Z. Hussain, S. Hussain, T. Kong, Z. Liu, Instability of mhd couette flow of an electrically conducting fluid, AIP Advances 8 (2018) 105209. doi:https://doi.org/10.1063/1.5051624.

[34] R. Kareem, J. Gbadeyan, Entropy generation and thermal criticality of generalized couette hydromagnetic flow of two-step exothermic chemical reaction in a channel, International Journal of Thermofluids 5 (2020) 100037. doi:https://doi.org/10.1016/j.ijft.2020.100037.

[35] E. Anyanwu, R. Olayiwola, M. Shehu, A. Lawal, Radiative effects on unsteady mhd couette flow through a parallel plate with constant pressure gradient, Asian Research Journal of Mathematics (2020) 1–19.

[36] I. Siddique, R. M. Zulqarnain, M. Nadeem, F. Jarad, Numerical simulation of mhd couette flow of a fuzzy nanofluid through an inclined channel with thermal radiation effect, Computational Intelligence and Neuroscience 2021 (2021). doi:https://doi.org/10.1155/2021/6608684.

[37] A. Akgül, I. Siddique, Analysis of mhd couette flow by fractal-fractional differential operators, Chaos, Solitons & Fractals 146 (2021) 110–893. doi:https://doi.org/10.1016/j.chaos.2021.110893.

[38] T. Sharma, P. Sharma, N. Kumar, Entropy generation in thermal radiative oscillatory mhd couette flow in the influence of heat source, in: Journal of Physics: Conference Series, volume 1849, IOP Publishing, 2021, p. 012023. doi:https://doi.org/10.1088/1742-6596/1849/1/012023.

[39] C. Owuor, Hydromagnetic Couette flow between two vertical semi-infinite permeable plates, Ph.D. thesis, JKUAT-COETEC, 2021.

[40] B. K. Jha, Y. J. Danjuma, Transient generalized taylor–couette flow of a dusty fluid: A semi-analytical approach, Partial Differential Equations in Applied Mathematics (2022) 100400. doi:https://doi.org/10.1016/j.padiff.2022.100400.

[41] B. K. Jha, P. B. Malgwi, Computational analysis on unsteady hydromagnetic couette flow of fluid—particle suspension in an accelerated porous channel, Partial Differential Equations in Applied Mathematics 5 (2022) 100370. doi:https://doi.org/10.1016/j.padiff.2022.100370.

[42] H.-S. Dou, Stability of taylor-couette flow between concentric rotating cylinders, in: Origin of Turbulence, Springer, 2022, pp. 271–304. doi:https://doi.org/10.1007/978-981-19-0087-7_9.

[43] W. Deng, J. Wu, P. Zhang, Stability of couette flow for 2d boussinesq system with vertical dissipation, Journal of Functional Analysis 281 (2021) 109255. doi:https://doi.org/10.1016/j.jfa.2021.109255.

[44] N. Masmoudi, B. Said-Houari, W. Zhao, Stability of the couette flow for a 2d boussinesq system without thermal diffusivity, Archive for Rational Mechanics and Analysis (2022) 1–108. doi:https://doi.org/10.1007/s00205-022-01789-x.